JOURNAL OF APPLIED PHYSICS 114, 024902 (2013)

Resonant ultrasound spectroscopy for a sample with cantilever boundary condition using Rayleigh-Ritz method

Farhad Farzbod[a)]
Google[x] Lab, Mountain View, California 94043, USA

(Received 5 April 2013; accepted 17 June 2013; published online 8 July 2013)

Resonant ultrasound spectroscopy (RUS) involves probing material properties by exciting and detecting resonant vibrational modes in a sample of interest. The desired material property is obtained by comparing theoretical and experimental results. Typically, the sample is considered to be freestanding with stress free boundary conditions. However in many situations of current interest, realizing a truly free sample is difficult. Here as an alternative, we consider a cantilever having a zero displacement boundary condition at one end of the sample. The eigenfrequencies and eigenmodes are obtained using a solution method that considers the exact equations of motion for an elastic sample. The solution is validated by comparing computed eigenfrequencies to a limiting case involving a long, thin sample. Additionally, a proof of principle experiment using laser-resonant ultrasound spectroscopy has been conducted on a copper cantilever. © *2013 AIP Publishing LLC*. [http://dx.doi.org/10.1063/1.4812758]

I. INTRODUCTION

Resonant ultrasound spectroscopy (RUS) is a characterization tool that involves relating material properties to the mechanical resonance response of a sample.[1–4] These properties include elastic constants,[5–10] dislocation density,[11] piezoelectric coefficients,[12] and crystallographic orientation.[13,14] In these applications, a free standing sample which is mechanically isolated from the environment is generally assumed. However, in many circumstances, the realization of a truly free standing specimen is difficult to achieve. For instance, in high temperature or high radiation environments,[15] manipulation and alignment of a remotely located sample can be extremely challenging. Mounting of sub-micron thick samples prepared using focused ion beam milling, provide another example.[16] For these cases, using a sample in the form of a cantilever is a preferable choice as it reduces the complication associated with sample mounting, manipulation and alignment.

Although RUS in its general form has been extensively used for a free sample, it has yet to be applied to a cantilever. Here, we present the theoretical development necessary to implement RUS on a cantilever. Our model considers a zero displacement boundary condition at one end of the sample. The solution, which is an adaptation of a model first presented by Visscher, considers the exact equations of motion for an elastic cantilever. Model results are validated by comparing computed eigenfrequencies to those predicted using classical beam theory for a long narrow sample. To illustrate the potential of this new approach, a proof of principle experiment, involving laser resonant ultrasound spectroscopy (LRUS), is carried out on a copper cantilever.

II. RUS FOR A CANTILEVER SAMPLE

A. Background

Vibration of a cantilever beam has been modeled by various methods. The most frequently applied methods employ Euler–Bernoulli and Timoshenko beam theory.[17] In these theories, a number of simplifying assumptions are made for the displacements of the sample making them best suited for lower order flexural modes.[18] While these two theories are an approximation, they suffice to model sample vibration relevant to several applications. Banerjee[19] used a dynamic stiffness formulation to model centrifugally stiffened Timoshenko beams. Murakami and Yamakawa[20] used a Timoshenko-type beam theory to study the dynamic response of plane anisotropic beams. Armstrong *et al.*[21] used the Euler-Bernoulli theory to investigate the effect of elastic anisotropy in copper. Other approximations have been utilized in this regard. Izumida *et al.*[22] used a thin shell theory to model beams at the micron and nanometer scales.

In other approaches, an energy functional of the system is formed using linear elasticity. In order to find the eigenfrequencies and eigenmodes of the system, one has to find a displacement function which minimizes the energy functional. A method to minimize this energy function was proposed by Ritz.[23] In this technique which is also referred to as the Rayleigh-Ritz method, the displacement function is stated as a linear combination of basis functions parameterized by unknown coefficients. Formulation of the eigenvalue problem is obtained by setting the derivatives of the energy functional with respect to each coefficient to zero. This method has been utilized in several applications. Of particular relevance to the work present here are applications involving RUS. For these applications, the resonant response is modeled by assuming a free standing sample.[1,3,12,24–26] Solution methods that use basis functions that conform to the geometry of the sample can be used to reduce the computational complexity. However, inexpensive and powerful modern processors have enabled the use of basis functions composed of polynomials. The advantage of this approach, first proposed by Visscher,[1] is that once coded a solution can be applied to any geometry with little alteration.

[a)]This research was performed while Farhad Farzbod was at Idaho National Laboratory, Idaho Falls, Idaho 83415, USA.

 © 2013 AIP Publishing LLC

Downloaded 15 Jul 2013 to 128.171.57.189. This article is copyrighted as indicated in the abstract. Reuse of AIP content is subject to the terms at: http://jap.aip.org/about/rights_and_permissions

In this paper, we use an adaptation of Visscher's method[1] to model vibrations of a cantilever sample. Because we take into account the cantilever boundary condition, a subset of the basis functions appropriate for a free sample is utilized. This method is explained in detail in Sec. II B.

B. RUS for a cantilever sample

The method we develop here can be applied to any sample geometry with one plane of zero displacement. In this subsection, we focus our attention on a cantilever sample with a rectangular cross-section. This enables us to compare this method to a limiting case based on the Euler–Bernoulli beam theory.

The sample geometry and the coordinate system are shown in Fig. 1. The deformation of the body u_i, can be stated in terms of an infinitesimal strain tensor

$$\varepsilon_{ij} = \frac{1}{2}\left[\frac{\partial u_i}{\partial x_j} + \frac{\partial u_j}{\partial x_i}\right], \quad i,j = 1,\ 2,\ 3. \tag{1}$$

Since the strain tensor is symmetric, the potential energy can be represented by

$$PE = \frac{1}{2} C_{ijkl} \frac{\partial u_i}{\partial x_j} \cdot \frac{\partial u_k}{\partial x_l}, \tag{2}$$

in which the Einstein summation convention is used. Assuming a sinusoidal time dependence with angular frequency ω, the Lagrangian is stated as

$$L = \frac{1}{2}\int_V \left(\rho\omega^2 u_i^2 - C_{ijkl}\frac{\partial u_i}{\partial x_j}\cdot\frac{\partial u_k}{\partial x_l}\right) dV, \tag{3}$$

where the integral is over the volume of the body. The boundary conditions for this configuration, see Fig. 1, can be categorized into two groups: natural boundary conditions and essential boundary conditions.[27] The natural boundary conditions, zero stress on the free surfaces and zero slope for the cantilevered end, are automatically satisfied upon finding a set of displacements which minimize the energy functional (3). In addition, the set of displacements must satisfy the essential boundary conditions:

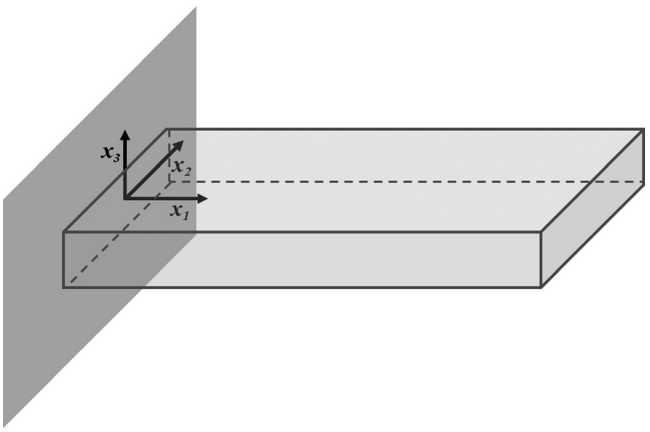

FIG. 1. Cantilever sample with coordinate system originated at a point on the center of the base.

$$u_i(0, x_2, x_3) = 0\,,\ i = 1,2,3. \tag{4}$$

At this stage, rather than seeking functions u_i in the space of continuous functions, we invoke the Ritz method by expanding the displacement vector using a complete set of basis functions

$$u_i = a_{iq}\varphi_q, \tag{5}$$

in which a_{iq} are the expansion coefficients and φ_{iq} are the basis functions. Similar to other numerical methods, only a subset of this complete set of functions is selected to represent u_i. As the cardinality of the subset increases, u_i approaches the correct solution. Following the approach of Visscher *et al.*,[1] we use polynomials as our basis functions. According to the Stone–Weierstrass theorem, the set of polynomials is dense in the space of continuous functions, meaning that the complete set of basis functions in Eq. (5) can be chosen as

$$\varphi_q(x) = x_1^l x_2^m x_3^n, \tag{6}$$

in which q is indexed by permutations of (l,m,n). Furthermore, in order to satisfy the essential boundary condition (4), we place a restriction on this set, namely,

$$\varphi_q(x) = x_1^l x_2^m x_3^n\ ,\ l \geq 1. \tag{7}$$

This condition restricts the set of polynomials to those with values that vanish at $x_1 = 0$. Nevertheless, this set is a complete set in the space of continuous functions that have zero value at $x_1 = 0$ (see the appendix). Using Visscher's method, only a subset of these basis functions is picked such that $l + m + n \leq \mathrm{N}$. Due to computational cost, we restrict our set to $\mathrm{N} = 11$, which is above the suggested value of 10.[1] Now by replacing u_i^2 with $\delta u_i u_{i'}$ in Eq. (3), then substituting Eq. (5) into Eq. (3), the Lagrangian can be rephrased as

$$L = \frac{1}{2}a_{iq}a_{i'q'}\rho\omega^2\int_V \delta_{ii'}\varphi_q(x)\varphi_{q'}(x)dV - \frac{1}{2}a_{iq}a_{kq'}\int_V C_{ijkl}\frac{\partial\varphi_q}{\partial x_j}\cdot\frac{\partial\varphi_{q'}}{\partial x_l}. \tag{8}$$

In a more compact form, Eq. (8) is expressed as:[3]

$$L = \frac{1}{2}(\rho\omega^2 \mathbf{a}^T\mathbf{E}\mathbf{a} - \mathbf{a}^T\mathbf{\Gamma}\mathbf{a}), \tag{9}$$

in which the matrices $\mathbf{E}$ and $\mathbf{\Gamma}$ represent volume integrals of products of the basis functions, their derivatives, and C_{ijkl}. The expansion coefficients, a_{iq}, are now expressed as vectors. Since the boundary condition is already satisfied by virtue of $l \geq 1$, invoking the Ritz method, we seek $\mathbf{a}$ such that L in Eq. (9) attains its extremum value. The necessary condition is satisfied by setting the derivative of L with respect to $\mathbf{a}$ to zero,

$$\rho\omega^2\mathbf{E}\mathbf{a} - \mathbf{\Gamma}\mathbf{a} = 0, \tag{10}$$

which is a general eigenvalue problem. In Sec. III, an example solution to this eigenvalue problem is presented.

Downloaded 15 Jul 2013 to 128.171.57.189. This article is copyrighted as indicated in the abstract. Reuse of AIP content is subject to the terms at: http://jap.aip.org/about/rights_and_permissions

III. RESULTS AND DISCUSSION

A. Eigenfrequencies and eigenmodes

In this subsection, we investigate the solution of a cantilever sample with a rectangular cross-section. The elastic properties used for calculation correspond to a highly textured copper sample that will be used in the subsequent proof of principle study. The stiffness tensor, measured previously,[28] has the following independent components: $C_{1111} = 174\,\text{GPa}$, $C_{1122} = 118\,\text{GPa}$, and $C_{2323} = 65\,\text{GPa}$. Using these tensor components, the eigenvalue problem (7) was solved numerically for various cantilever lengths of fixed 2.0 mm width by 0.5 mm thickness. Eigenfrequencies are tabulated in Table I and the eigenmodes are depicted in Figure 2. In Table I, we also tabulated resonant frequencies obtained using Euler–Bernoulli beam theory. The relation between the elastic stiffness tensor components and Young's modulus (along the axis of the cantilever) used in the Euler Bernoulli theory is given by

$$E_{11} = C_{1111} - C_{1122} + \frac{C_{1122}(C_{1111} - C_{1122})}{C_{1111} + C_{1122}}. \tag{11}$$

As is evident, there are frequencies missing in the Euler-Bernoulli theory. The latter theory merely calculates eigenfrequencies with bending eigenmodes. As is apparent in Figure 2(b), the second and fifth eigenmodes are not bending modes in the x_3 direction for a 17 mm sample. Eigenfrequencies in Table I also illustrate that as the length of the sample gets longer, eigenfrequencies obtained by the method developed here, on average approach the ones calculated by Euler-Bernoulli theory.

B. Boundary condition

A central issue with any RUS experiment involves ensuring that the boundary conditions are properly satisfied. For traditional RUS experiments great care is taken in mounting the sample so as to minimize acoustic coupling to the environment. Similarly for a cantilever, it is important to design a holding apparatus such that the cantilever boundary condition is realized. For this purpose, conventional RUS with piezoelectric transducers is not an appropriate choice to excite and/or detect vibrations. On the other hand, noncontact RUS eliminates acoustic coupling between the transducer and the specimen, making it a suitable choice to serve this purpose. This would also enable RUS to be performed *in situ* in harsh environments. Methods to implement noncontact RUS include electromagnetic acoustic transducers[29] and laser ultrasound.[15,25,26,28] In LRUS, both excitation and detection of sample vibrations are performed by lasers. Ultrasonic waves are thermoelastically generated in a sample by a laser and on the detection side an interferometer is used to detect vibrations. By raster scanning the probe laser, an image of the displacement pattern associated with each eigenfrequency (i.e., eigenmode) can be obtained.[25,26,28] Given that laser spots can be focused to a few microns, it is also possible to perform LRUS on micron scale samples.

Ensuring the proper boundary condition at the clamped end can be achieved by using LRUS in two ways. First, by verifying locations of nodal points, according to Euler-Bernoulli method,[30] these nodal points of each out of plane bending eigenmode are geometric properties of the beam. Using LRUS, the nodal points can be located with ease. However, care has to be taken regarding modes we choose for this test. As it can be seen in Figs. 2(a) and 2(b), these modes change their location in the frequency spectrum as the length of the beam varies, i.e., it is not guaranteed that the fourth eigenmode is a bending mode. Second by raster scanning the surface of the beam and mapping the eigenmodes, we are able to verify both the displacement and its derivative vanish at the clamped end.

As a proof of concept, we performed LRUS on a cantilever sample. The cantilever used in this study was machined from a highly textured copper sheet using electron discharge

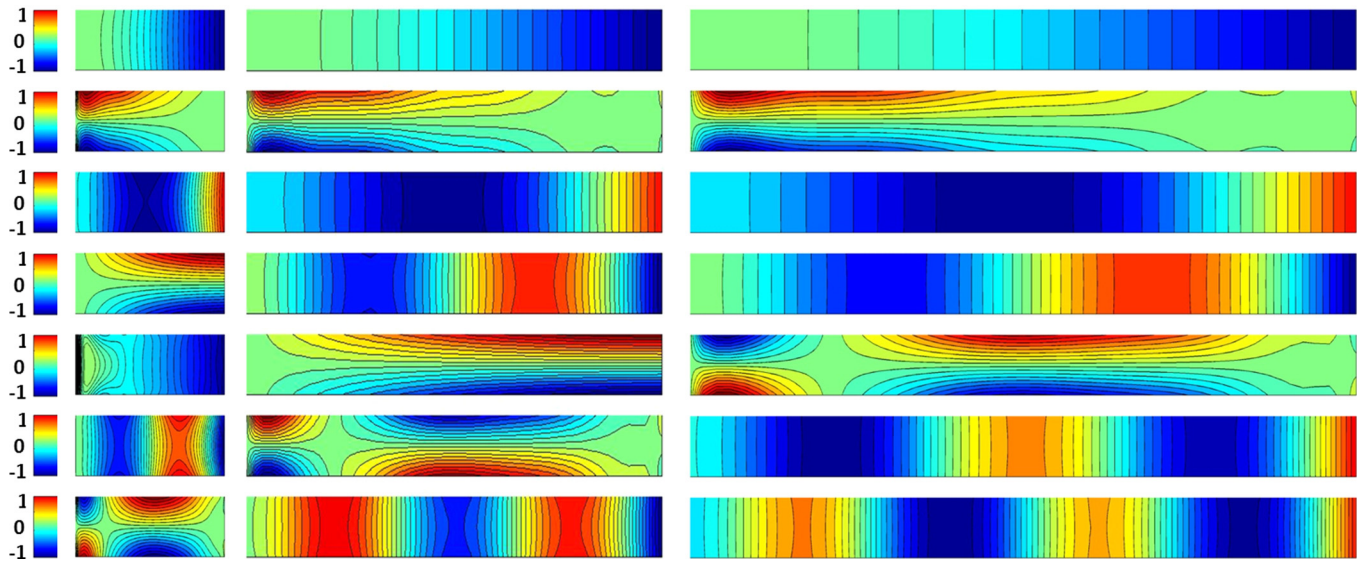

FIG. 2. In (a), (b), and (c) eigenmodes for out of plane motion in the direction of x_3 is depicted for 5, 17, and 50 mm samples, respectively. In (a), 2nd, 4th, 5th, and 7th modes are torsional modes, while in (b), torsional modes are in the 2nd, 5th, and 6th place, and in (c), they are 2nd and 5th modes. Sample sizes are not to scale in the figure.

Downloaded 15 Jul 2013 to 128.171.57.189. This article is copyrighted as indicated in the abstract. Reuse of AIP content is subject to the terms at: http://jap.aip.org/about/rights_and_permissions

TABLE I. Eigenfrequencies for various sample lengths with 2 × 0.5 mm rectangular cross-section calculated by Euler-Bernoulli formalism and the numerical solution to the exact problem (denoted by N method). The average differences between two methods are 2.57%, 2.09%, and 1.38% for 5, 17, and 50 mm samples, respectively.

5mm			17 mm			50 mm		
N method (Hz)	Euler-Bern. (Hz)	Difference (%)	N method (Hz)	Euler-Bern. (Hz)	Difference (%)	N method (Hz)	Euler-Bern. (Hz)	Difference (%)
10013	9582	4.30	848	829	2.24	97	96	1.03
36707			3338	0		387		
60771	60047	1.19	5304	5194	2.07	609	600	1.48
63973			14836	14544	1.97	1706	1681	1.47
150866			18050	0		2417		
164490	168134	2.22	20179	0		3346	3295	1.52
172328			29060	28504	1.91	5538	5446	1.66

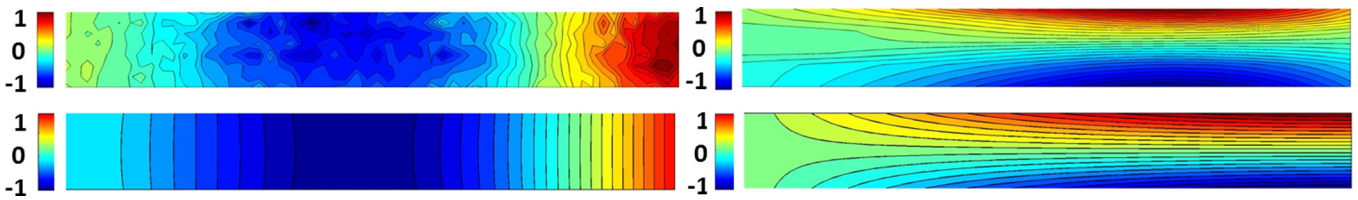

FIG. 3. Experimental (on the top) and theoretical (on the bottom) eigenmodes for 17 × 2 × 0.5 mm copper sample. The theoretical modes are the third and the fifth modes in Figure 2(b).

machining. The cantilever dimensions are 17 × 2 × 0.56 mm and the components of the elastic stiffness tensor are given in the Sec. III A. A holder made out of steel was used to secure the sample in place and imposing zero displacement at the clamped end. A pulsed neodymium-doped yttrium aluminum garnet (Nd:YA G) laser operating at 1064 nm was used to thermoelastically excite broadband resonant ultrasonic modes in the sample. A commercial Bossa-Nova photorefractive interferometer operating at 532 nm is used to record the out-of plane surface motion associated with ultrasonic resonances. Experimental mode shapes are constructed by raster scanning the probe beam on a 60 × 9 point grid on the surface of the sample and then mapping the frequency-domain response. Two representative experimental eigenmodes are shown in the top of Fig. 3. The left side of the image corresponds to the second flexural mode and the right side corresponds to the second torsional mode. The corresponding theoretical eigenmodes are shown on the bottom of Fig. 3. The normalized, with respect to the maximum, experimental displacement at the cantilever base is 0.0594 for the torsional mode. This nonzero displacement at the base translates to discrepancy between theoretical frequency of 19815 Hz and experimental frequency of 18357 Hz for the torsional mode.

For the inverse problem, meaning extracting the elastic stiffness tensor from the LRUS data, we can follow the same routine developed by Migliori *et al.*[2] involving Levenberg–Marquardt numerical scheme. Pursuing the inverse problem will be the subject of future work.

IV. CONCLUSION

A theoretical technique, based on the exact equations of motion, was developed to calculate eigenfrequencies and eigenmodes of an elastic cantilever. This technique was validated by comparing calculated eigenfrequencies to a limiting case involving a long, thin beam. This theoretical development for the cantilever boundary paves the way to perform inverse problem in which we extract the elastic stiffness tensor from the measured eigenfrequencies. A proof of concept experiment using laser-resonant ultrasound spectroscopy has been conducted on a copper cantilever to measure two eigenmodes.

APPENDIX: STONE-WEIERSTRASS THEOREM IN CASES WITH CANTILEVER BOUNDARY CONDITION

Let u be a continuous function for every $x = (x_1, x_2, x_3) \in \boldsymbol{D} = [a_1,b_1] \times [a_2,b_2] \times [a_3,b_3]$. By the Weierstrass approximation theorem, we have: For every $\varepsilon > 0$, there exists a polynomial function p over $\mathbf{R}^3$ such that for all x in $\boldsymbol{D}$, we have $\|u(x) - p(x)\|_\infty < \varepsilon$. Now let $a_1 = 0$ and $u(0, x_2, x_3) = 0$. We want to show that the set of polynomials $p'(x)$ with $p'(0, x_2, x_3) = 0$ approximates $u(x)$ on $\boldsymbol{D}$.

For each ε, by the Weierstrass theorem, we pick $p(x)$ such that $\|u(x) - p(x)\|_\infty < \varepsilon/2$. Then $p(x) = p'(x) + \sum_{m,n} x_2^m x_3^n$ for some polynomials $p'(x)$. Since the norm is the supreme norm, we have $\|u(0, x_2, x_3) - p'(0, x_2, x_3) - \sum_{m,n} x_2^m x_3^n\| < \varepsilon/2$ and since $u(0, x_2, x_3) = p'(0, x_2, x_3) = 0$, we have $\| \sum_{m,n} x_2^m x_3^n\| < \varepsilon/2$. Now,

$$\begin{aligned} ||u(x)-p'(x)||_\infty &= ||u(x)-p(x) + \Sigma_{m,n} x_2^m x_3^n||_\infty \\ &\le ||u(x)-p(x)||_\infty + ||\Sigma_{m,n} x_2^m x_3^n||_\infty \\ &\le \varepsilon/2 + \varepsilon/2 = \varepsilon. \end{aligned}$$

[1]W. M. Visscher, A. Migliori, T. M. Bell, and R. A. Reinert, J. Acoust. Soc. Am. **90**(4), 2154–2162 (1991).

Downloaded 15 Jul 2013 to 128.171.57.189. This article is copyrighted as indicated in the abstract. Reuse of AIP content is subject to the terms at: http://jap.aip.org/about/rights_and_permissions

[2]A. Migliori, J. L. Sarrao, W. M. Visscher, T. M. Bell, M. Lei, Z. Fisk, and R. G. Leisure, Physica B **183**(1–2), 1–24 (1993).
[3]R. G. Leisure and F. A. Willis, J. Phys. Condens. Matter **9**(28), 6001–6029 (1997).
[4]A. Migliori and J. D. Maynard, Rev. Sci. Instrum. **76**(12), 121301 (2005).
[5]M. Radovic, E. Lara-Curzio, and L. Riester, Mater. Sci. Eng., A **368**(1–2), 56–70 (2004).
[6]N. Nakamura, H. Ogi, and M. Hirao, J. Appl. Phys. **111**(1), 013509 (2012).
[7]J. J. Adams, D. S. Agosta, R. G. Leisure, and H. Ledbetter, J. Appl. Phys. **100**(11), 113530 (2006).
[8]J. Tian, H. Ogi, T. Tada, and M. Hirao, J. Acoust. Soc. Am. **115**(2), 630–636 (2004).
[9]H. Seiner, L. Bodnarova, P. Sedlak, M. Janecek, O. Srba, R. Kral, and M. Landa, Acta Mater. **58**(1), 235–247 (2010).
[10]H. Seiner, P. Sedlak, L. Bodnarova, A. Kruisova, M. Landa, A. de Pablos, and M. Belmonte, J. Acoust. Soc. Am. **131**(5), 3775–3785 (2012).
[11]F. Barra, A. Caru, M. T. Cerda, R. Espinoza, A. Jara, F. Lund, and N. Mujica, Int. J. Bifurcation Chaos Appl. Sci. Eng. **19**(10), 3561–3565 (2009).
[12]H. Ogi, N. Nakamura, K. Sato, M. Hirao, and S. Uda, IEEE Trans. Ultrason. Ferroelectr. Freq. Control **50**(5), 553–560 (2003).
[13]J. L. Sarrao, S. R. Chen, W. M. Visscher, M. Lei, U. F. Kocks, and A. Migliori, Rev. Sci. Instrum. **65**(6), 2139–2140 (1994).
[14]F. Farzbod and D. H. Hurley, IEEE Trans. Ultrason. Ferroelectr. Freq. Control **59**, 2470 (2012).
[15]R. S. Schley, K. L. Telschow, J. B. Walter, and D. L. Cottle, Nucl. Technol. **159**(2), 202–207 (2007).
[16]J. McCarthy, Z. Pei, M. Becker, and D. Atteridge, Thin Solid Films **358**(1–2), 146–151 (2000).
[17]S. M. Han, H. Benaroya, and T. Wei, J. Sound Vib. **225**(5), 935–988 (1999).
[18]H. E. Rosinger and I. G. Ritchie, J. Test. Eval. **2**(3), 131–138 (1974).
[19]J. R. Banerjee, J. Sound Vib. **247**(1), 97–115 (2001).
[20]H. Murakami and J. Yamakawa, J. Eng. Mech. **123**(12), 1268–1275 (1997).
[21]D. E. J. Armstrong, A. J. Wilkinson, and S. G. Roberts, J. Mater. Res. **24**(11), 3268–3276 (2009).
[22]W. Izumida, Y. Hirayama, H. Okamoto, H. Yamaguchi, and K. J. Friedland, Phys. Rev. B **85**, 075313 (2012).
[23]W. Ritz, J. Reine Angew. Math. **135**(1/4), 1–5 (1909).
[24]G. X. Liu and J. D. Maynard, J. Acoust. Soc. Am. **131**(3), 2068–2078 (2012).
[25]D. H. Hurley, S. J. Reese, and F. Farzbod, J. Appl. Phys. **111**(5), 053527 (2012).
[26]S. J. Reese, K. L. Telschow, T. M. Lillo, and D. H. Hurley, IEEE Trans. Ultrason. Ferroelectr. Freq. Control **55**(4), 770–777 (2008).
[27]R. G. Bartle, *The Elements of Real Analysis*, 2nd ed. (Wiley, 1976).
[28]D. H. Hurley, S. J. Reese, S. K. Park, Z. Utegulov, J. R. Kennedy, and K. L. Telschow, J. Appl. Phys. **107**(6), 063510 (2010).
[29]H. Ogi, H. Ledbetter, S. Kim, and M. Hirao, J. Acoust. Soc. Am. **106**(2), 660–665 (1999).
[30]Y. M. Tseytlin, Rev. Sci. Instrum. **76**(11), 115101 (2005).

Downloaded 15 Jul 2013 to 128.171.57.189. This article is copyrighted as indicated in the abstract. Reuse of AIP content is subject to the terms at: http://jap.aip.org/about/rights_and_permissions